



Role of Al(OH)₃ Nanocatalyst on Hydrogen Generation from Al/H₂O Reaction Medium

M. VENNILA*, G. JAYAPRIYA^{id} and T. MAHESWARI^{id}

PG and Research Department of Chemistry, Government Arts College, Dharmapuri-636705, India

*Corresponding author: E-mail: vennilaraja@gmail.com

Received: 17 February 2021;

Accepted: 28 July 2021;

Published online: 20 September 2021;

AJC-20514

Aluminum hydroxide nanoparticles were synthesized using sodium aluminate (NaAlO₂) solution and varying amounts of ethanol and methanol under different reaction conditions. The synthesized nanoparticles were characterized using XRD, FESEM and FTIR techniques. The synthesized aluminium hydroxide nanoparticles employed as a catalyst to generate hydrogen from Al/H₂O reaction medium. The maximum hydrogen generation with 100% efficiency achieved within 1.50 h at 1:1:200 ratio of Al:Al(OH)₃:H₂O. This mode of hydrogen generation was collective, non-hazardous, non-corrosive and very promising alternate fuel for energy system.

Keywords: Nanocatalyst, Aluminum hydroxide, Hydrogen generation, Hydrolysis reaction.

INTRODUCTION

Aluminium readily reacts with water, which is important to the development of heat and hydrogen gas [1]. Recently, it was reported that hydrogen gas was generated at room temperature from the reaction of aluminum nanoparticles using tap water [2].

An efficient and developed method of generating hydrogen, which acts as fuel and alternate energy system to the hydrogen energy technologies to fulfil growing demand for alternative energy sources. Generation of hydrogen from Al/H₂O reaction (hydrolysis reaction) has been of scientific interest in recent years [3-6]. The corrosive aluminum metal in aqueous solutions has long remained recognized as a good way to a generation of hydrogen [1].

Other applications of aluminum and water reactions consume developed, including Al/H₂O “green” propellants, which possess a definite compulsion of around 230 s due to the graceful weightiness hydrogen gas [7-9]. The individual thermal quantity of the hydrogen energy analogous with the Al/H₂O reaction is normally used around 65% of hydrogen gas. Hydrogen gas is a fresh and clean fuel cell with a high energy density 119.8 MJ kg⁻¹. However, its volumetric energy density is slightly reduced at 0.01 MJ L⁻¹ [10].

Generally, aluminum powder and the stimulated aluminum are exposed to atmosphere and environment. It remained to

establish that there is an active degradation when the aluminum was deposited in air through definite moisture for a while then the mechanism is not clear [11-16]. The Al/H₂O reaction promoted by a synthetically prepared Al(OH)₃ nanoparticles deferment established that the interaction between aluminum and Al(OH)₃ particles and the reaction heat are two key factors in development of the mechanism of the reaction. Actually, in this studies, a rapid generation of hydrogen can be recognized by using synthesized Al(OH)₃ nanosized powders [17-19]. Aluminum hydroxide was found to be unique and powerful catalysts for the generation of hydrogen from an Al/H₂O system at a low cost.

The product of Al/H₂O reaction is Al(OH)₃, which is simply reprocessed to produce aluminum by Halle-Heroult process [20]. Though, a great activity of Al/H₂O reaction is forbidden by a thin layer of Al₂O₃ on its surface of aluminum powder. The hydrogen generation can be accomplished by consuming a neutral solution. The mechanisms of the Al/H₂O reactions on the measure of a particular reacting particle and particularly at impressive densities have not been consistently recognized. A protecting natural surface layer of alumina is well-known to smother the reaction at room temperature and a number of inquiries motivated on the elimination of this protecting layer.

In this current study, the best amalgamation and a mixture of Al:Al(OH)₃:H₂O was framed to generate hydrogen. The

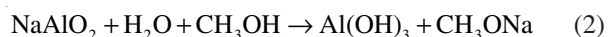
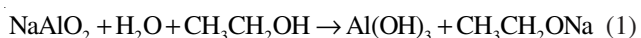
synthesized Al(OH)₃ nanoparticles was confirmed to be identical effective catalysts to promote hydrogen generation from Al/H₂O system consisted of very small, fine particle size and of low crystallinity. To improve the efficiency of synthesized Al(OH)₃ nanoparticles, the different precursors were sourced to synthesize nanoparticles. The 100% efficiency of hydrogen production was achieved (1,360 mL/g Al at 25 °C) from neutral water within 2 h using Al(OH)₃ nanocatalyst.

EXPERIMENTAL

All the chemicals were of reagent grade and used as received without further purifications. Sodium aluminate (NaAlO₂), ethanol, methanol were purchased from Merck, India. Double distilled water was used throughout this study.

Characterization: The powder XRD analysis was performed using a Bruker D8 PHASER powder diffraction instrument equipped with a K α radiation of copper target as the light source and an acrylic sample holder. The morphologies of the samples were characterized using a field-emission scanning electron microscope (FESEM) and Fourier transform infrared spectra (FTIR).

Synthesis of aluminum hydroxide nanoparticles: The nanostructured aluminum hydroxide nanoparticles was synthesized using an ethanol and methanol precipitation method. Initially, NaAlO₂ (2 and 5 g) was dissolved in 30-150 mL of deionized water and stirred continuously until dissolution completed. Then, various amounts of precipitating agent such as ethanol/methanol was gradually added into the NaAlO₂ solution and stirred 250 rpm for 10 h (Table-1). The white precipitate was centrifuged, washed with water and dried at 70 °C for 24 h. The chemical reaction for the precipitation of Al(OH)₃ can be described in following eqn. 1:



RESULTS AND DISCUSSION

Aluminium hydroxide nanoparticles exist in two phases *viz.* Gibbsite and Bayerite were confirmed the X-ray diffraction

studies. Table-1 presents the obtained crystal phase and the reaction conditions for aluminium/water. Aluminium powders do not undergo a reaction with water, where oxide layers are present on corners of the surface. The time required for complete aluminium hydration with water was estimated. For pure solutions, good results were achieved. Various combinations of NaAlO₂ with methanol and ethanol were analyzed to study the hydrogen generation effect.

XRD studies: Before and after annealing, the XRD patterns of the sample are given in Fig. 1. The powder XRD patterns of Al(OH)₃ nanocatalysts synthesized from different amounts of precipitating agents (ethanol and methanol) and sodium aluminate solution is presented in Fig. 2. The prepared Al(OH)₃ nanocatalysts exhibited two phases: bayerite phase (2 θ 18.3446°, 20.3566°) and gibbsite phase (2 θ 18.3137°, 20.2956°, 20.5434°). The peaks of the X-ray diffraction pattern are compared with the available standard JCPDS data to confirm the crystal structure. In the spectra, the major reflections were acceptable for the nanocatalysts of Al(OH)₃; however, some low intensity peaks were observed. Small peaks were obtained due to the existence of hydrated sodium aluminate [13].

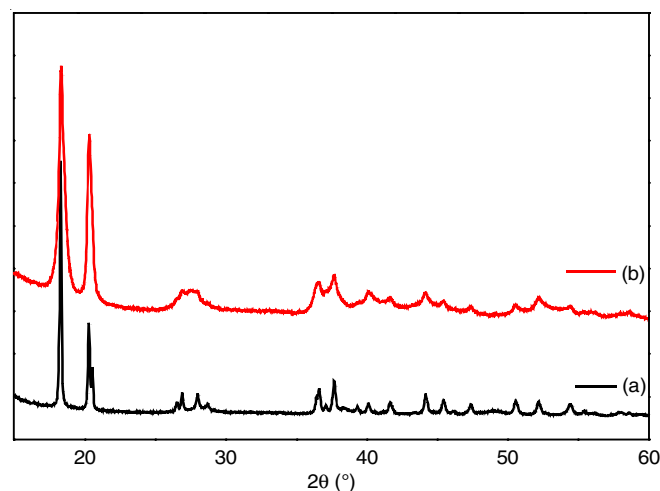


Fig. 1. XRD pattern of Al(OH)₃ nanoparticles prepared a 2 °C (a) from methanol, (b) from ethanol

TABLE-1
STUDY CONDITIONS OF THE SYNTHESIZED Al(OH)₃ NANOPARTICLES

Sample-ID	NaAlO ₂ (g)	Ethanol (mL)	H ₂ O (mL)	Crystal phase	Temp (°C)
Sample-1	2.0	1400	150	Bayerite	Room temperature
Sample-2	2.0	1500	150	Bayerite	Room temperature
Sample-3	2.0	1600	150	Bayerite	Room temperature
Sample-4	2.0	1600	150	Bayerite	Ice bath
Sample-5	5.0	1400	150	Bayerite	Room temperature
Sample-6	2.0	400	30	Gibbsite	Ice bath
Sample-7	2.0	400	50	Gibbsite	Ice bath
Sample-8	2.0	400	100	Bayerite	Ice bath
Sample-9	2.0	400	150	Bayerite	Ice bath
Sample-10	2.0	400	30	Bayerite	Room temperature
Sample-11	2.0	400	50	Bayerite	Room temperature
Sample-12	2.0	400	100	Bayerite	Room temperature
Sample-13	2.0	400	150	Bayerite	Room temperature
Sample-14	5.0	400	50% hot + 50% cold	Gibbsite	Room temperature
Sample-15	5.0	400 Methanol	150	Gibbsite	Room temperature

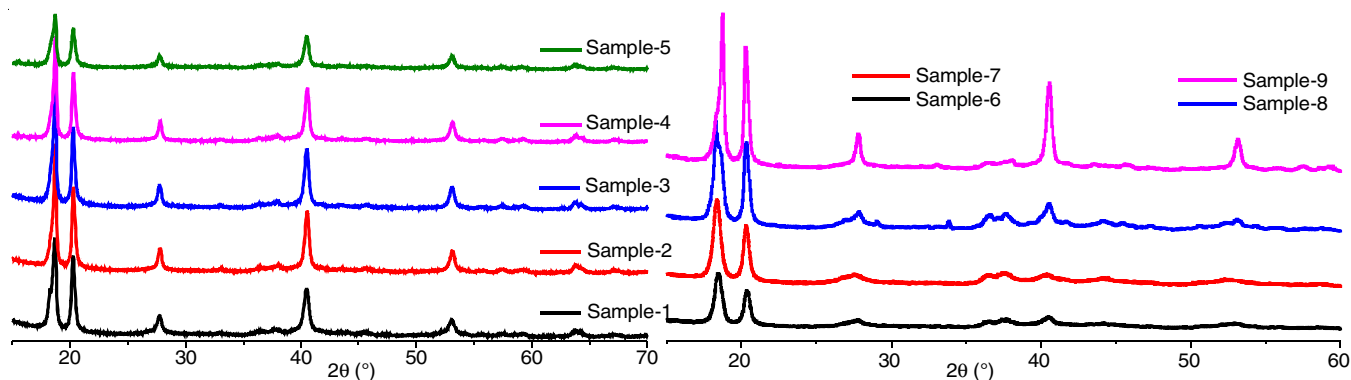


Fig. 2. XRD pattern of synthesized $\text{Al}(\text{OH})_3$ nanoparticles (samples S1-S9)

FESEM studies: Fig. 3 illustrates the FESEM images of the prepared $\text{Al}(\text{OH})_3$ nanopowders. Samples S2-S5 nanoparticles exhibit crystal-like morphology and sample S1 shows the fine spherical and rod-shaped (hexagonal) particles. The sample S2-S5 have a high ethanol/water mole ratio and NaAlO_2 concentration (Table-1). These conditions lead to spherical and crystal particle formation. The size of sample S5 nanoparticles (high NaAlO_2 concentration) is the same as that of samples S1-S4 nanoparticles. The size of samples S1-S5 range 40-85 nm. The width of the rod-like particles of sample S1 is large.

Samples S6-S9 nanoparticles are small, with crystal-like, rod-shaped and particulate-like morphology. Catalysts must have this type of structures because it can provide extra active sites for catalytic reactions. Different arrangements of the FESEM images of samples S6-S9 are shown in Fig. 4.

Fig. 5 presents the FESEM image of the $\text{Al}(\text{OH})_3$ catalysts. The stretching microstructure of all particles is well preserved

and glowing. In both catalysts, the microstructure of $\text{Al}(\text{OH})_3$ nanoparticles was standardized and smooth, and the type particles size obtained at different temperatures were similar.

FTIR studies: Fig. 6 presents the FTIR spectra of the prepared $\text{Al}(\text{OH})_3$ nanoparticles in $4000\text{-}400\text{ cm}^{-1}$. The broad band appearing at 3629 cm^{-1} represents the stretching vibration of the O-H group. The sharp absorption band obtained at 3531 and 1544 cm^{-1} can be attributed to the $\nu(\text{-OH})$ and $\nu(\text{NO})$ stretching vibrations. The FTIR spectra were effectively used to determine the functional groups of the samples. The peak observed at 527 cm^{-1} corresponds to $\text{Al}(\text{OH})_3$ stretching vibrations.

Hydrogen generation using $\text{Al}(\text{OH})_3$: In the prepared $\text{Al}(\text{OH})_3$ powders, hydrogen improvement is highly effective (Fig. 7). Using the exothermic reaction of $\text{Al}/\text{H}_2\text{O}$ systems, we accelerated 100% hydrogen yield by employing a large amount of metal Al powders. The $\text{Al}(\text{OH})_3$ effectively enhances

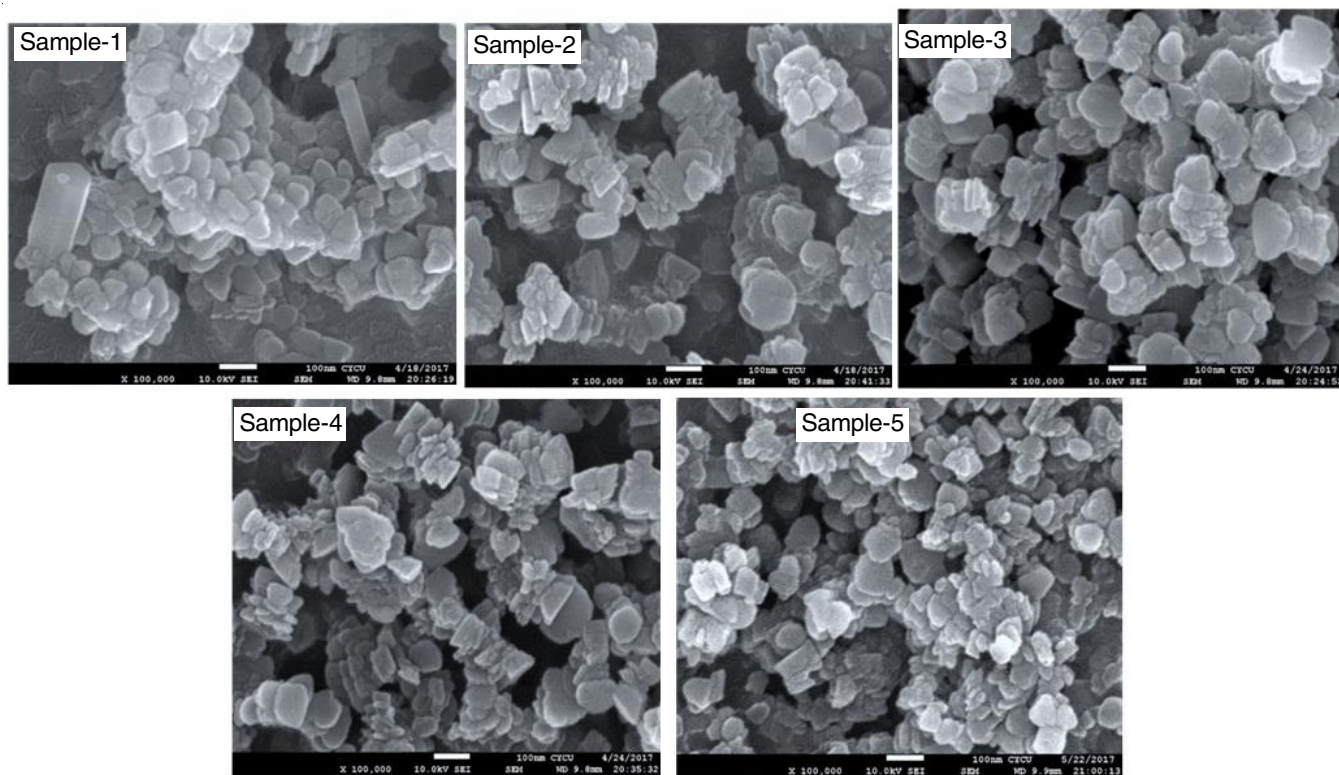


Fig. 3. FESEM images aluminum hydroxide nanoparticles of samples S1-S5

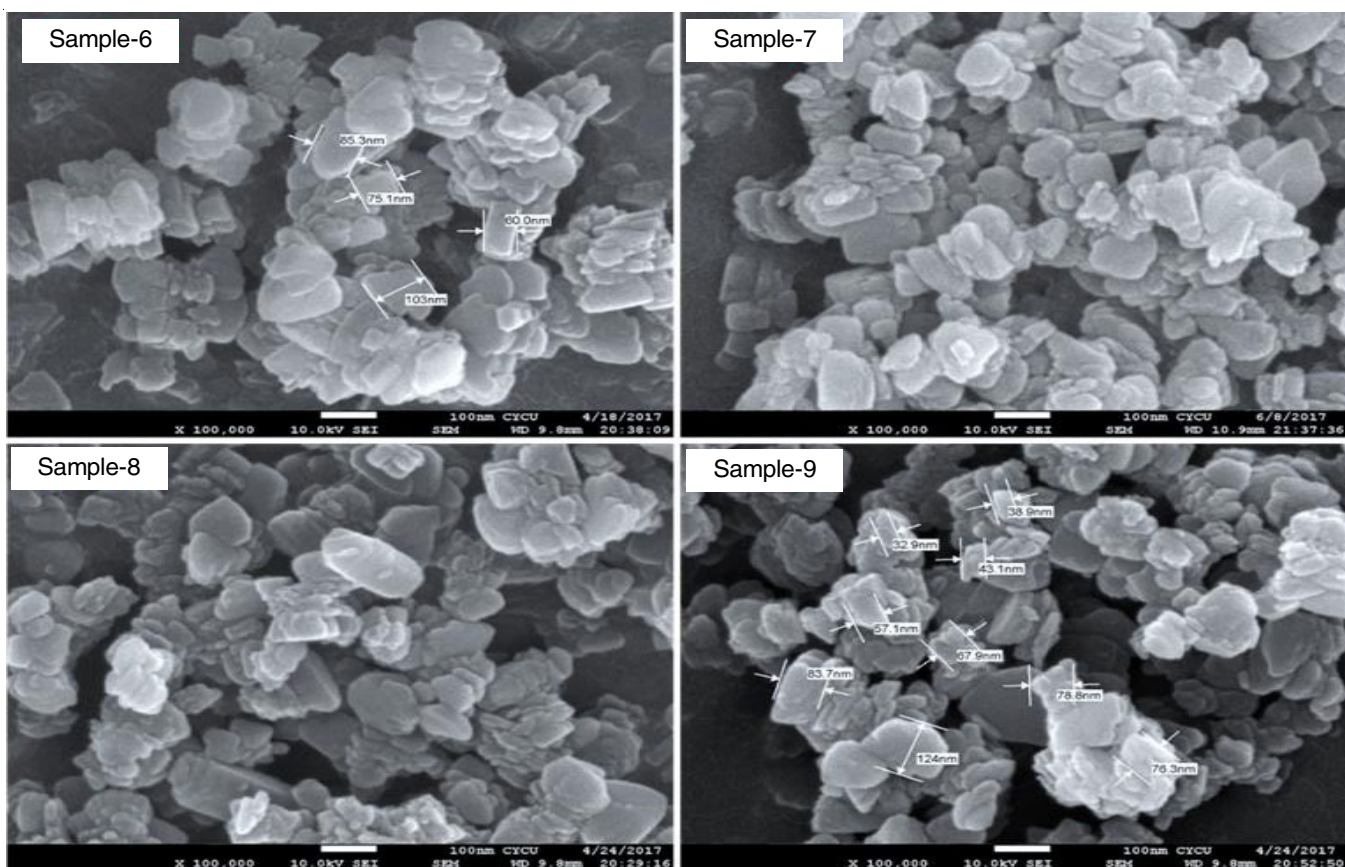
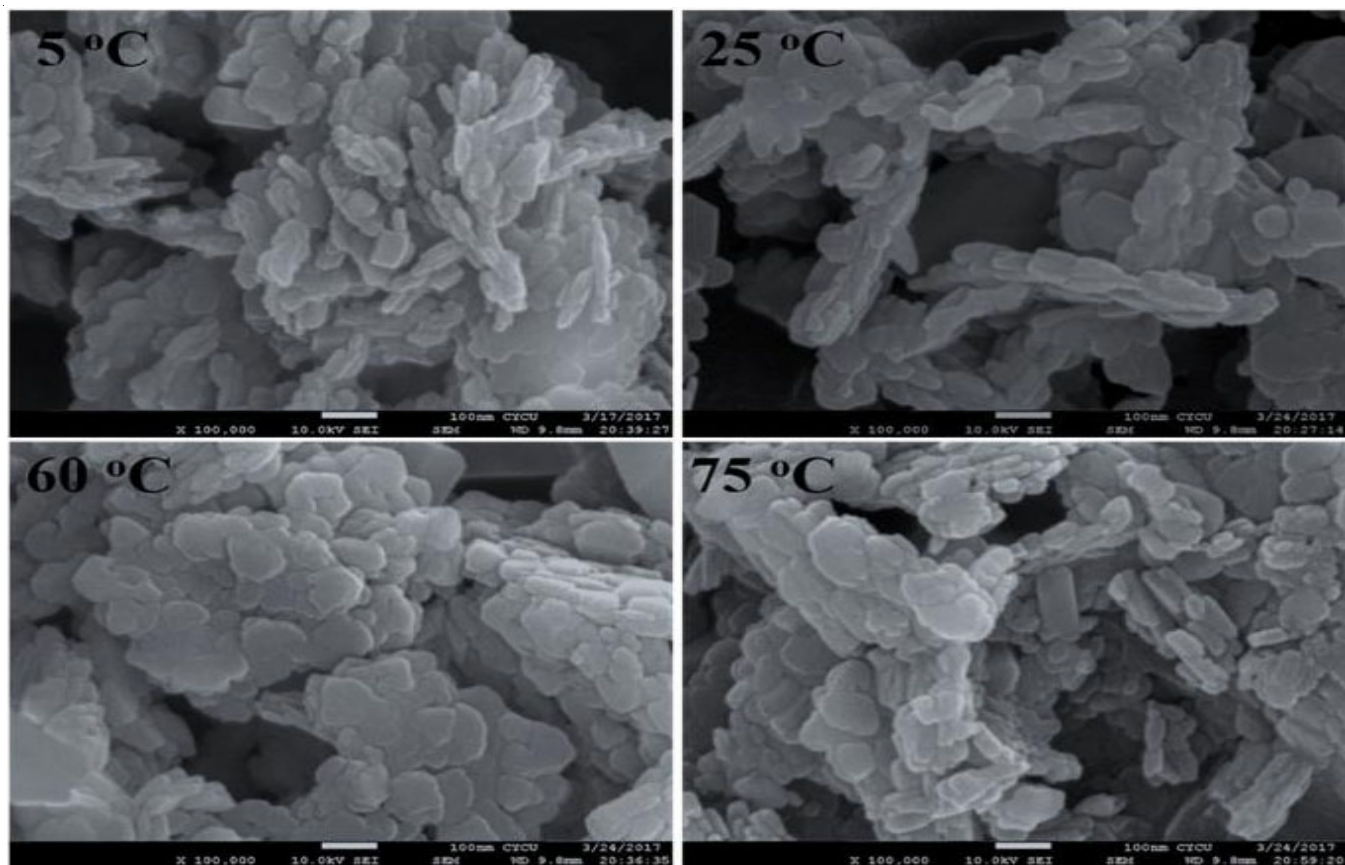


Fig. 4. FESEM images aluminum hydroxide nanoparticles of samples S6-S9

Fig. 5. FESEM images of synthesized $\text{Al}(\text{OH})_3$ at different temperatures

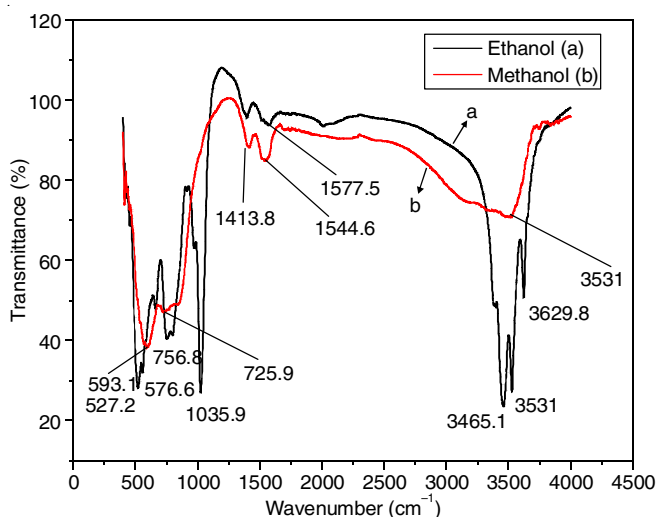


Fig. 6. FTIR spectra of Al(OH)₃ nanoparticles from ethanol and methanol precursors

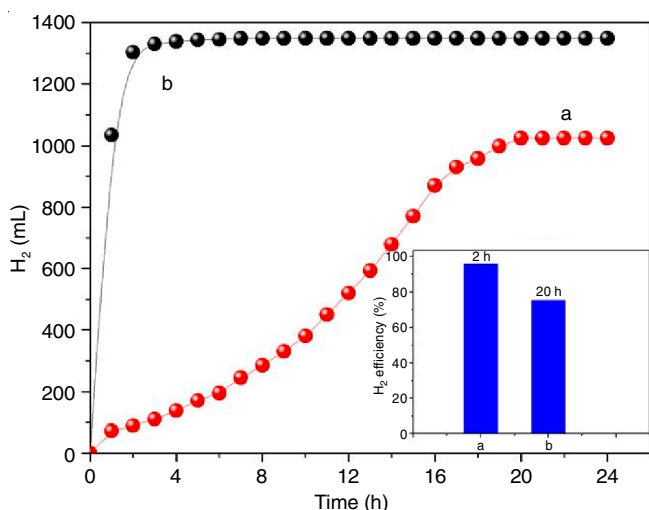


Fig. 7. Volume of the generated gas (H₂) versus time for the hydrolysis of Al and H₂O reaction. Using Al(OH)₃ catalysts (a) from methanol, (b) from ethanol. Inset: Corresponding efficiency values of the catalysts

hydrogen generation from the Al/H₂O system, whereas other precursors are less effective for hydrogen generation.

The cost-effective catalysts are highly improved for hydrogen production from reaction of water and Al hydrolysis ($2\text{Al} + 6\text{H}_2\text{O} \rightarrow 2\text{Al}(\text{OH})_3 + 3\text{H}_2$). In this study, the improved Al(OH)₃ (S1-S5) exhibited as a highly organized catalytic effect and were active for water and Al hydrolysis (Fig. 8). The hydrolysis of water and Al by using samples S1-S5 Al(OH)₃ nanoparticles was completed within 1 h (83.96-99.99% catalytic performance). For the Al and water hydrolysis, the Al(OH)₃ nanoparticles efficiency achieved was higher than that of the methanol-synthesized Al(OH)₃ catalysts, which indicated a high activity of Al(OH)₃ powders.

As-fabricated Al(OH)₃ nanoparticles were used as catalysts for water and Al hydrolysis. The reaction was initiated at room temperature (25 °C) by treating water and Al in the reaction flask containing Al(OH)₃ nanoparticles. The catalytic effect of Al(OH)₃ was determined by employing the water-filled gas burette method. Samples S8 and S9 of Al(OH)₃ nanoparticles

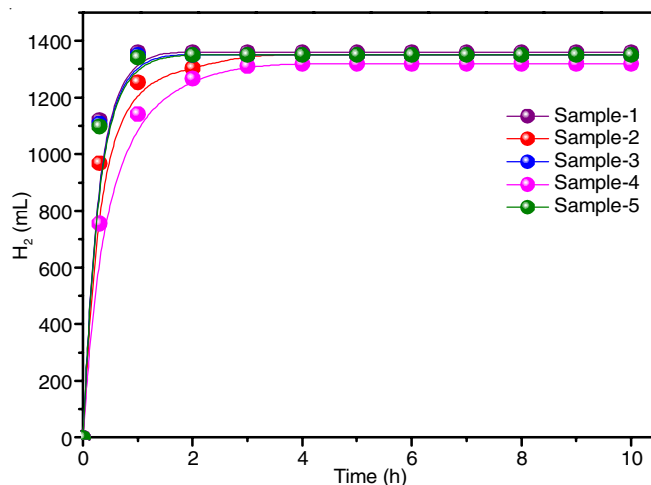


Fig. 8. Volume of the generated gas (H₂) versus time for the hydrolysis of Al and H₂O reaction using Al(OH)₃ catalysts (Samples S1-S5)

catalysts exhibited a considerably high catalytic activity for water and Al hydrolysis (Fig. 9). The amount of hydrogen generated increased with the increase in Al(OH)₃ and the time of reaction affected molar ratio (samples S8 and S9) of catalysts and catalysts. In the presence of Al(OH)₃ catalysts, a stoichiometric volume of hydrogen was generated through water and Al hydrolysis within 1 h (89.19-93.17%).

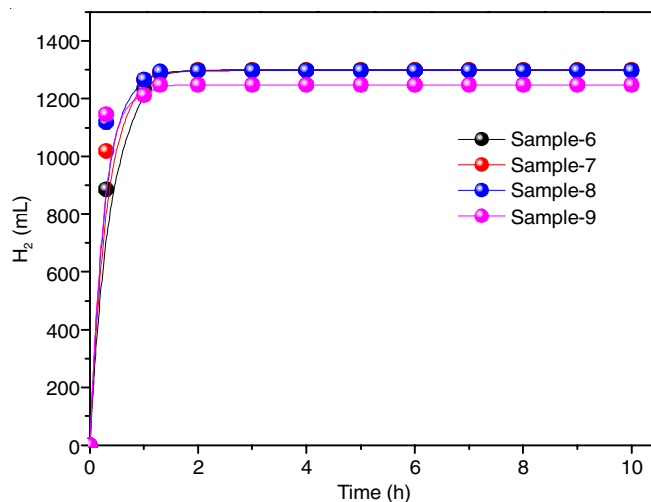


Fig. 9. Volume of the generated gas (H₂) versus time for the hydrolysis of Al and H₂O reaction using Al(OH)₃ catalysts (Samples S6-S9)

For the curves, the difference in temperatures was 5-150 °C. Figs. 8 and 9 show the changes in of H₂ gas particle generation with time and related images, respectively. The curves evolved for aluminium nanoparticles hydrolysis. The hydrogen production yield and hydrolysis rate enhanced with the temperature increase. In 1 h, hydrolysis led to up to 100% production of theoretical amount of hydrogen. When reaction temperature decreased to 5 °C, then the hydrolysis rate decreased. Moreover, the final hydrogen yield also decreased.

Conclusion

Hydrogen generated by hydrolysis aluminium hydroxide nanoparticles was studied. In addition to hydrogen generation,

the Al/water reaction could be employed to produce alumina and Al(OH)₃ nanoparticles for various applications. For hydrogen generation, the optimum Al/Al(OH)₃/water combination was obtained with the synthesized Al(OH)₃ nanoparticles, *i.e.* samples S6, S5 and S9, whose size was < 50 nm. For Al/water reaction, the catalytic effect of Al(OH)₃ nanoparticles was likely based on a few properties of Al(OH)₃ nanoparticles, such as large surface area, high-energy active sites, fine and small particles. Spherical and fine particles exhibited a high catalytic activity because of their high-energy sites near plate edges. By using the self-heating exothermic reaction in minimum water with a large amount of Al powder, rapid hydrogen generation (yield 100%) and high temperature can be achieved, which renders this system an ideal hydrogen source for use-on-demand systems.

CONFLICT OF INTEREST

The authors declare that there is no conflict of interests regarding the publication of this article.

REFERENCES

- Z. Gao, F. Ji, D. Cheng, C. Yin, J. Niu and J. Brnic, *Energies*, **14**, 1433 (2021); <https://doi.org/10.3390/en14051433>
- S. Prabu and H.-W. Wang, *Catal. Sci. Technol.*, **11**, 4636 (2021); <https://doi.org/10.1039/D1CY00534K>
- H.Z. Wang, D.Y.C. Leung, M.K.H. Leung and M. Ni, *Renew Sustain. Energy Rev.*, **13**, 845 (2009); <https://doi.org/10.1016/j.rser.2008.02.009>
- H.S. Yoo, H.Y. Ryu, S.S. Cho, M.H. Han, K.S. Bae and J.H. Lee, *Int. J. Hydrogen Energy*, **36**, 15111 (2011); <https://doi.org/10.1016/j.ijhydene.2011.08.061>
- L. Soler, J. Macanas, M. Munoz and J. Casado, *J. Power Sources*, **169**, 144 (2007); <https://doi.org/10.1016/j.jpowsour.2007.01.080>
- L. Soler, A.M. Candela, J. Macanas, M. Munoz and J. Casado, *Int. J. Hydrogen Energy*, **35**, 1038 (2010); <https://doi.org/10.1016/j.ijhydene.2009.11.065>
- G.A. Risha, Y. Huang, R.A. Yetter, V. Yang, S.F. Son and B.C. Tappan, *AIAA Paper*, 1154 (2006).
- T.F. Miller and J.D. Herr, *AIAA Paper*, 3788 (2004).
- A. Ingenito and C. Bruno, *J. Propuls. Power*, **20**, 1056 (2004); <https://doi.org/10.2514/1.5132>
- G. Thomas and C. San Ramon, Overview of storage development DOE Hydrogen Program, Sandia National Laboratories; p. 9 (2000).
- O.V. Kravchenko, K.N. Semenenko, B.M. Bulychev and K.B. Kalmykov, *J. Alloys Compd.*, **397**, 58 (2005); <https://doi.org/10.1016/j.jallcom.2004.11.065>
- A. V. Ilyukhina, O.V. Kravchenko, B.M. Bulychev and E.I. Shkolnikov, *Int. J. Hydrogen Energy*, **35**, 1905 (2010); <https://doi.org/10.1016/j.ijhydene.2009.12.118>
- J.T. Ziebarth, J.M. Woodall, R.A. Kramer and G. Choi, *Int. J. Hydrogen Energy*, **36**, 5271 (2011); <https://doi.org/10.1016/j.ijhydene.2011.01.127>
- X.Y. Chen, Z.W. Zhao, X.H. Liu, M.M. Hao, A.L. Chen and Z.Y. Tang, *J. Power Sources*, **254**, 345 (2014); <https://doi.org/10.1016/j.jpowsour.2013.12.113>
- X.Y. Chen, Z.W. Zhao, M.M. Hao and D.Z. Wang, *J. Power Sources*, **222**, 188 (2013); <https://doi.org/10.1016/j.jpowsour.2012.08.078>
- Y.A. Liu, X.H. Wang, H.Z. Liu, Z.H. Dong, S.Q. Li, H.W. Ge and M. Yan, *Energy*, **89**, 907 (2015); <https://doi.org/10.1016/j.energy.2015.06.043>
- H.T. Teng, T.Y. Lee, Y.K. Chen, H.W. Wang and G. Cao, *J. Power Sources*, **219**, 16 (2012); <https://doi.org/10.1016/j.jpowsour.2012.06.077>
- Y.K. Chen, H.T. Teng, T.Y. Lee and H.W. Wang, *Int. J. Energy Environ. Eng.*, **5**, 87 (2014); <https://doi.org/10.1007/s40095-014-0087-3>
- H.W. Wang and M.S. Chin, *Int. J. Chem. Eng. Appl.*, **6**, 146 (2015); <https://doi.org/10.7763/IJCEA.2015.V6.470>
- L. Soler, A.M. Candela, J. Macanas, M. Munoz and J. Casado, *Int. J. Hydrogen Energy*, **34**, 8511 (2009); <https://doi.org/10.1016/j.ijhydene.2009.08.008>